Hybrid polymeric electrolyte based on methylalumoxane

M. Piszcz, M. Marczewski, A. Plewa-Marczewska, G.Z. Żukowska, A. Zalewska,
A. Pietrzykowski, M. Siekierski*

Polymer Ionics Research Group, Warsaw University of Technology, Chemical Faculty, Noakowskiego 3, PL-00664 Warsaw, Poland

ARTICLE INFO

ABSTRACT

In this article the properties of the electrolyte based on the product of the reaction of methylalumoxane with oligoethyleneglycols are examined. The electrochemical studies were performed to describe the conductivity and lithium transference number of the system. In addition, DSC, SEM, NMR and vibrational spectroscopy studies were used to get a more detailed description of the material. Three classes of electrolytes are here taken into consideration. The first based on the PEGDME liquid oligoether system modified with the MAO–PEGME branched heterocomposite system. The second one is the branched product itself used as an electrolyte matrix. In the last case a crosslinked system was obtained by the utilization of PEGME–PEG mixture. The conductivities obtained were in the range of 10^{-4} S cm^{-1} for liquid-like systems and above 10^{-5} S cm^{-1} for the solid ones. For samples containing LiCF$_3$SO$_3$ the lithium transference number was higher than 0.5 for some electrolyte compositions while it was in the range of 0.4 for ones containing LiClO$_4$. Electrochemical stability of the system was preliminarily tested by means of cyclic voltammetry.

1. Introduction

Independently of 30 years of research devoted to the development of polymeric electrolytes based on polyethyleneoxide this group of compounds is still very attractive as a starting point for synthesis of new ionically conductive materials. One of the reasons for this fact is that polyethyleneoxide (PEO) based electrolytes are well-known systems [1–9] which gives a good starting point for understanding of behavior of more complicated systems. The most important problem observed in the PEO-based electrolytes is related to low overall ionic conductivity at ambient temperature explained by the presence of the crystalline phase in the polymer matrix. In addition, the fraction of charge transported by cations is about 0.3 due to high anion mobility in the system.

There are a few possible ways of solving this problem. One of them developing the general idea of Composite Polymer Electrolyte (CPE) [10–13]. Another possible way of solving this problem was developed based on the direct obtaining of the filler through an *in situ* chemical process. Depending on the applied chemistries and process conditions the inorganic part can form physically dispersed filler grains [14], semi-interpenetrating network [15] or be chemically bonded to organic groups forming an inorganic–organic polymer [16]. The range of the precursors applied leading to the inorganic part formation is very wide [17–22].

E.g. Armand et al. [23] obtained an organo-mineral proton-conducting polymer which has a silicate frame with different organic functional group "grafts" with it.

It is worth noting that an interesting group of structures can be obtained from compounds which contain aluminum atoms in their structure. For this element the possibility of structure forming is combined with strong Lewis acid properties of the electron-deficient aluminum atom. In consequence, it is additionally able to change ionic equilibriums present in the system through interactions with anions. For example LiAlH$_4$ [24,25], alkoxy compounds (isopropoxy [26], butoxy [27]), triethylaluminum [28], aluminum carboxylate [29] as well as alumoxanes [30] were used in hybrid CPE as inorganic phase precursors.

E.g. Di Noto et al. [31] present aluminum-containing hybrid inorganic–organic polymer electrolytes. In this case aluminum isopropoxide and PEG 400 were used as precursors.

Al$((OCH_2CH_2)_nOCH_3)_3$ was used as an additive to solid polymer electrolytes [32]. This receptor exhibits similar thermal (between 200 and 300 °C) and electrochemical (4.2 V vs. Li/Li$^+$ at 60 °C and 4.5 V at RT) stability as analogous boron receptors and polyethers. Also in analogy to boron receptors, its addition resulted in higher conductivity of the system due to plasticization (lower T_g for a receptor-containing system was measured) [33].

Zygadło-Monikowska and coworkers [34] prepared electrolytes starting from triethylaluminum and poly(ethylene glycol) methyl ethers with average molecular mass from 120 to 350. In another paper Zygadło-Monikowska et al. [29] presented another compos-

* Corresponding author. Tel.: +48 22 234 5739; fax: +48 22 628 2741.
E-mail address: alex@ch.pw.edu.pl (M. Siekierski).

ite electrolyte based on organoaluminum compound. In this case the precursor was based on aluminum carboxylate.

In the present paper a novel class of composite electrolytes based on organometallic precursor capable of reacting with oligoether compounds forming a hybrid polymer matrix is investigated. Contrastively to the works presented above a novel idea of using methylalumoxane as a precursor forming branched or crosslinked hybrid organic–inorganic CPE systems is introduced here. In this case each unit originating from the organometallic precursor does not consist of single aluminum nuclei, but forms itself nanoscale oxyaluminum cluster. This molecule contains in its outer shell (see Fig. 1) up to twelve Al–C bonds able to act as the reactive sites. In our other paper [35] we show the details of matrix formation reaction in terms of stoichiometry and coordination changes. The purpose of MAO application is pointed here for not only preparing a polymeric matrix with low concentration of highly ordered polymeric regions but also to obtaining systems of evenly distributed nanosized Al–O clusters. So prepared matrix is used in this work to prepare heterocomposite electrolytes containing lithium salts.

2. Experimental

2.1. Reactants

Trimethylaluminum 2.0 M in toluene (Aldrich) was used as received. Methylalumoxane was synthesized according to the procedure described in Ref. [36]. PEGME of average molecular weight 350, 750 and 1000 (Aldrich/Fluka) and PEG of average molecular weight 200, 300, 400 and 1000 were dried at $100\,^\circ$C for 72 h under vacuum (10^{-5} Torr) prior to be used and stored in an argon filled dry box. PEGDME M_{w} = 500 g mol^{-1} (Aldrich) was dried in the identical way. Toluene (POCH) was dried by refluxing over potassium benzophenonate. Anhydrous toluene-d8 (Aldrich) was used as received. LiCF$_3$SO$_3$ and LiClO$_4$ (Aldrich) were also vacuum dried prior to use.

2.2. Synthesis

The PEGME was dropped as the pure reagent into the methylalumoxane solution in toluene at room temperature. After 1 h of stirring the mixture was warmed to $50\,^\circ$C and kept in this temperature for 2 h. Then the toluene was distilled off under reduced pressure and the residue was kept for analysis. The reactions of methylalumoxane with PEGME were carried out with the molar ratio equal to 1:2, 1:4, 1:6, 1:8 and 1:12. The salt used was previously dissolved in the PEGME. In the case of crosslinked systems the reaction was carried out in two steps. One was identical to the previously described while in the other PEG (crosslinking agent) was added.

2.3. Conductivity measurements

Ionic conductivity was determined by means of impedance spectroscopy. The electrolytes were pressed between stainless-steel blocking electrodes. A VMP 3 Multichannel electrochemical analyzer was used in 1 Hz to 500 kHz frequency range. The cell was immersed in a HAAKE DC 50 cryostat to control the measurement temperature in -20 to $70\,^\circ$C range. A Bernard Boukamp EQ software [37] was used to analyze the obtained impedance data.

2.4. Transference number determination

The experiments were performed on a VMP 3 Multichannel electrochemical analyzer. The lithium ion transference numbers (t_{Li^+}) of the membrane samples were measured at a fixed temperature ($25\,^\circ$C). The steady-state (polarization) technique, which involves a combination of AC- and DC-measurements, was applied [38–40]. The impedance response of the Li|electrolyte|Li cell was measured prior to the DC-polarization run, in which a small voltage pulse (ΔV) was applied to the cell until the polarization current reached the steady-state I_{ss}. Finally, the impedance response of the cell was measured again. The double AC test was required to determine electrolyte resistance (R_{e}) as well as the solid-electrolyte interphase (SEI) resistance before (R_0) and after (R_{ss}) DC-polarization. That allowed evaluation of the initial current (I_0) arising immediately ($\sim$10 μs at $50\,^\circ$C) after the application of the voltage, since, along with the Ohm's law, $I_0 = \Delta V/(R_{\mathrm{e}} + R_0)$. According to this method, the transference number t_{Li^+} of lithium ions, as the carriers of charge flowing through the Li|solid-electrolyte|Li cell, could be calculated through the following
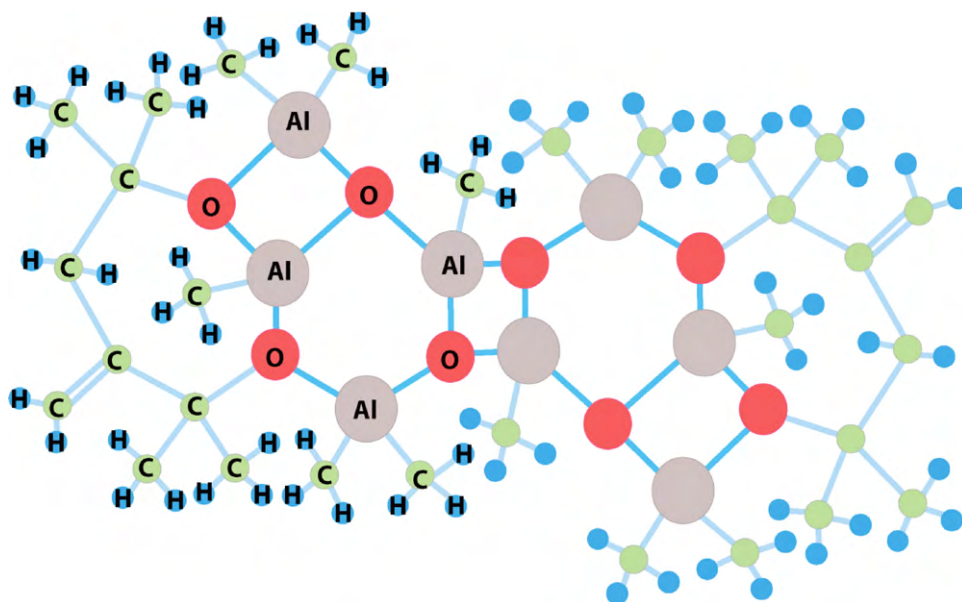

Fig. 1. Molecular structure of methylalumoxane.

equation:

$$t_+ = \frac{I_s}{I_0} \cdot \frac{\Delta V - I_0 R_0}{\Delta V - I_s R_s}$$

where R_0, initial SEI resistance of passive layers formed at both lithium electrodes; R_{ss}, secondary passive layer resistance (as the steady-state polarization current is reached).

2.5. Cyclic voltammetric studies

Cyclic voltammetric studies of the hybrid polymer electrolytes were carried out on golden metal working electrode ($0.0314\,cm^2$) in a three electrode cell in which Tantalium wires served as both the counter and the reference electrodes. In the analyzed system the potential of the tantalum quasi reference is about +0.05 V towards SHE. VMP 3 Multichannel electrochemical analyzer was used to perform the voltammetric experiments. Only multibranched electrolytes as a viscous liquid were tested. Samples were tested in different range potentials and different scan speeds.

2.6. DSC

The DSC data were collected using a DSC Q200 at the heating rate of $5\,°C\,min^{-1}$ at 0–$250\,°C$ temperature range (crystallinity measurements) and, after this measurement, at the heating rate $20\,°C\,min^{-1}$ at -120 to $0\,°C$ temperature range (glass transition temperature measurements).

2.7. FT-IR spectroscopy

The FT-IR spectra were obtained on a Perkin Elmer System 2000 FT-IR spectrometer. The FT-IR spectra of liquid samples were recorded in the 4000–$600\,cm^{-1}$ spectral range for thin liquid films pressed between NaCl plates. For solid compounds the spectra were obtained using an ATR Golden Gate facility, equipped with diamond crystal and ZnSe lenses. The spectral resolution was $2\,cm^{-1}$; each spectrum was averaged from 32 scans.

2.8. Raman spectroscopy

The Raman spectra were recorded on a Nicolet Almega Dispersive Spectrometer equipped with a confocal microscope. The samples were placed in sealed glass vials. In general the spectra were recorded using the 532 nm excitation line and 2400 lines grating. Only for MAO–PEGME or MAO–CH_3OH adducts a 780 nm line was used. The exposition time varied from 20 to 45 s, when the 532 nm laser was used to 180 s for experiments performed using the 780 nm laser. The spectral resolution was about $4\,cm^{-1}$.

2.9. ^1H and ^{27}Al NMR measurements

^1H and ^{27}Al NMR spectra were recorded on a computer interfaced Varian VNMRS 500 MHz spectrometer with VnmrJ 2.2c Software at 499.94 MHz and 130.27 MHz respectively. All measurements were performed at $25\,°C$. The spectra were analyzed using MestReNova-5.2.5 software. The samples were dissolved in toluene-d8 (99.6 at.% D, anhydrous, Aldrich). The reference for ^1H NMR was TMS, for ^{27}Al NMR the reference was signal from aluminum acetylacetonate. In all the cases quartz
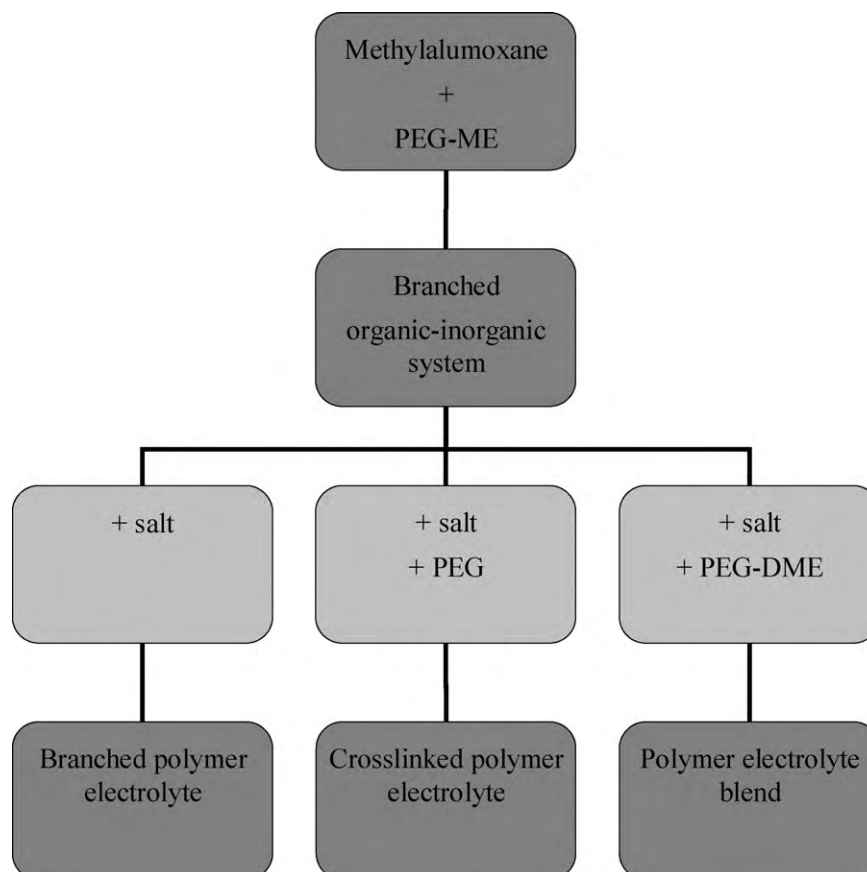

Fig. 2. Reaction steps for obtaining hybrid polymer electrolytes.

Table 1
Sample composition, constitution (just after reaction and after ageing), lithium ion transference number and DSC data.

Sample	Non-crosslinked systems										DSC data		
	Mol PEG 200/1MAO	Mol PEG 300/1MAO	Mol PEG 1000/1MAO	Mol PEGME 350/1MAO	Mol PEGME 750/1MAO	Mol PEGME 1000/1MAO	Mol PEGDME 500/1MAO	wt% MAO	Constitution/ ageing	$t_+=$	T_g [°C]	T_{cryst} [°C]	T_m [°C]
PEG 350	–	–	–	1	–	–	–	–	Liquid	–	–	–	
OD100	4	–	–	6	–	–	–	–	Liquid	–	–	–	
I T2	–	–	–	8	–	–	310	0.35	Liquid	0.56	−64.2	−36.8	7.75
I T5	–	–	–	8	–	–	120	0.9	Liquid	0.57	–		
II T2	–	–	–	8	–	–	310	0.35	Liquid	0.51	–		
II T5	–	–	–	8	–	–	120	0.9	Liquid	0.52	–		
I P2	–	–	–	8	–	–	311	0.35	Liquid	0.32	–		
II P2	–	–	–	8	–	–	125	0.35	Liquid	0.33	–		
I P5	–	–	–	8	–	–	312	0.9	Liquid	0.31	–		
II P5	–	–	–	8	–	–	125	0.9	Liquid	0.23	–		
R11120	–	–	–	12	–	–	–	12.5	Liquid	–	−68.6	−33.7	−6.4
R11080	–	–	–	8	–	–	–	19	Liquid	–	−61.7	–	–

Sample	Crosslinked systems									DSC data		
	Mol PEG 200/1MAO	Mol PEG 300/1MAO	Mol PEG 1000/1MAO	Mol PEGME 350/1MAO	Mol PEGME 750/1MAO	Mol PEGME 1000/1MAO	wt% MAO	Constitution/ ageing	$t_+=$	T_g [°C]	T_{cryst} [°C]	T_m [°C]
R1100	4	–	–	6	–	–	16.3	Liquid/solid	–	–	–	–
R1182350/300	–	2	–	8	–	–	14.9	Liquid	–	–	–	–
R1162350/300	–	2	–	6	–	–	18.8	Rubbery	–	–	–	–
R1142350/300	–	2	–	4	–	–	24.7	Solid	–	–	–	–
R162350/200	2	–	–	6	–	–	20	Liquid	–	–	–	–
R142350/200	2	–	–	4	–	–	26.7	Solid	–	–	–	–
R162750	2	–	–	6	–	–	11.3	Solid	–	–	–	–
R142750	2	–	–	4	–	–	16.2	Solid	–	–	–	–
R0821000/1000	–	–	2	–	–	8	–	Solid	–	43.6	−9.6	39
R1821000/100	–	–	2	–	–	8	5.6	Solid	–	−47.2	−12	35.8 and 47.4

2.10. SEM studies

Scanning Electron Microscope (SEM) Quanta200 was used to examine the morphology of hybrid polymer electrolytes. 20 kV acceleration voltage was used with magnification for EDAX equal 5000× and distribution of S, Al, O, and C nucleus was investigated.

3. Results and discussion

The systems studied based on the MAO organometallic precursor can be divided into three main groups (Fig. 2). The first one, where systems utilize the product of the reaction of mono-capped oligoether (of various M_w being in range 350–1000 g mol^{-1})

with MAO as the only constituent of the polymeric matrix. In this case the samples are characterized not only by changing molecular weight of the organic compound but also by the varying amount of Al–CH$_3$ moieties undergoing the reaction with the –OH groups. In the second case the reaction is carried out in two steps. The second group of electrolytes is obtained in reaction of a branched system with PEG molecules containing two –OH moieties—in this situation PEG acts as crosslinking agent. Contrary to the first situations where a viscous liquid was formed, in the later case the consistency of the sample varies from liquid through rubbery to brittle solid depending on the M_w of the organic compounds and the sample composition. In the third case a polymer blend is obtained by mixing PEGDME ($M_w = 500$ g mol^{-1}) with the product of chemical reaction of MAO with PEGME ($M_w = 350$ g mol^{-1}). In this case the first oligoether compound does not contain in its structure any free –OH moieties and, in consequence, does not take part in chemical
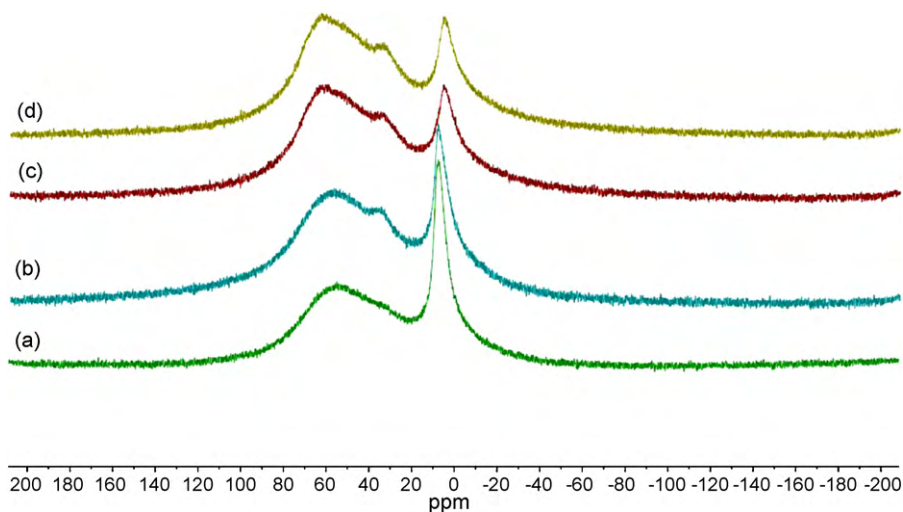

Fig. 3. The ^{27}Al NMR spectra of the product of reaction of methylalumoxane with PEGME and PEG in molar ratio equal to 1:4:2: (a) without lithium triflate, (b) with an addition of lithium triflate, (c) sample "b" after one week of storage, and (d) sample "b" after two weeks of storage.
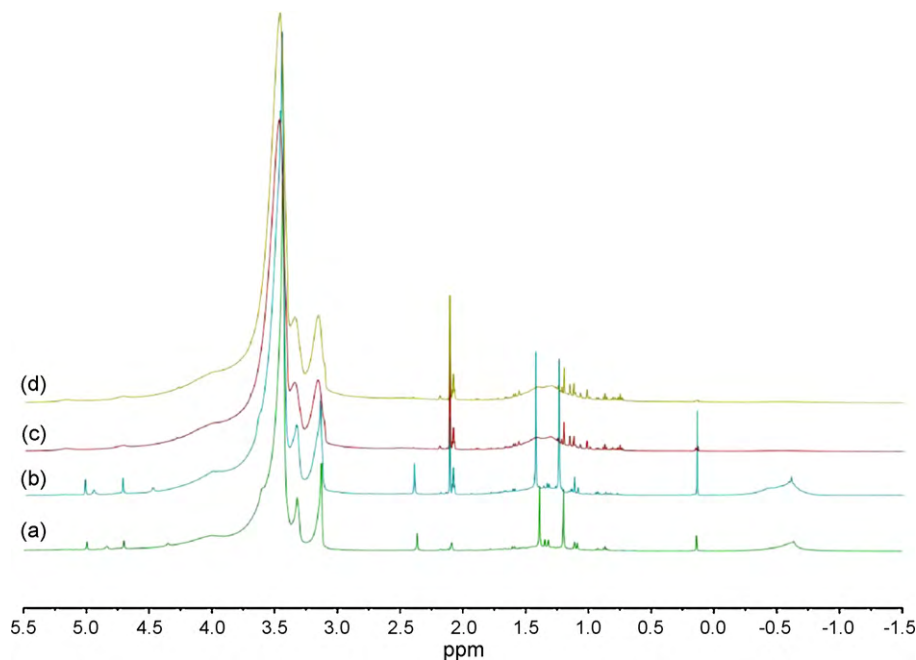

Fig. 4. The ^{1}H NMR spectra of the product of reaction of methylalumoxane with PEGME and PEG in molar ratio equal to 1:4:2: (a) without lithium triflate, (b) with an addition of lithium triflate, (c) sample "b" after one week of storage, and (d) sample "b" after two weeks of storage.
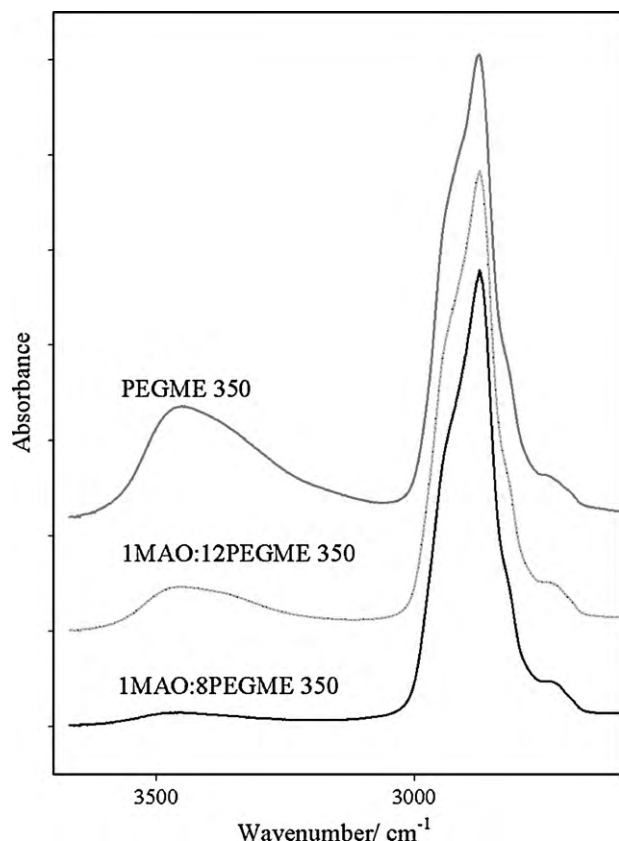
Fig. 5. Effect of diminishing of the OH signal observed in the FT-IR spectra of PEGME 350–MAO systems.

interactions with the MAO molecule. Studied sample compositions were gathered in Table 1.

3.1. NMR studies

To investigate the behavior of a sample of electrolyte after synthesis and during storage, the products of reaction of methylalumoxane with PEGME and PEG in molar ratio equal to 1:4:2 were studied using ^{27}Al NMR and ^{1}H NMR spectroscopy. As the examination of heterocomposite matrix itself was described in our other paper [35], we concentrate here only on differences in system behavior originating from salt addition. Just after the reaction,

in ^{27}Al NMR spectrum (Fig. 3a and b) one can notice the appearance of signals originated from a six-coordinated aluminum atom located at 7.6 ppm for the sample without lithium triflate and at 8.2 ppm for the sample with the addition of salt. The shape of the background signal suggests that there are also five-coordinated aluminum atoms in the sample. After the measurements the sample with lithium triflate was heated up to 80 °C and stirred for 5 h and then stored for one week in ambient conditions. After one week of storage the measurements were performed again (Fig. 3c) and it was observed that the chemical shift of the six-coordinated aluminum atom changed to 5 ppm. It can be explained by the interaction of lithium triflate with aluminum atoms. After another week of storage a ^{27}Al NMR spectrum (Fig. 3d) of the sample was made and it looked almost the same as the latter one. In the ^{1}H NMR the decrease of signal located between −1.0 and −0.2 ppm corresponding to hydrogens from methyl groups bonded with aluminum atoms during the storage is observed (Fig. 4). This suggests that after a period of time, methylalumoxane reacts with all –OH groups presented in the reactant mixture. At the beginning, the lithium triflate possibly interacts with terminal –OH groups of PEG which renders the reaction with methylalumoxane impossible.

3.2. Vibrational spectroscopy studies

As was stated in our other paper [35] spectral analysis confirmed the reaction of MAO with hydroxyl groups of polyethylene glycol The decrease in hydroxyl groups density is related to a change in relative intensities of bands attributed to ν_{SO_3} of triflate "free anions" (1032 cm^{-1}) and "ionic pairs" (1039 cm^{-1}). The intensity of the latter is higher in MAO modified samples than for the reference PEGME–LiCF$_3$SO$_3$ system, which is in agreement with influence of hydroxyl groups on the dissociation of lithium salts in PEO low molecular weight analogues.

Unfortunately, in the spectra of both electrolytes, the only spectral feature which can be ascribed to MAO adducts is the weak and broad band between 650 and 720 cm^{-1}, corresponding to Al–O stretching vibrations, which makes a direct analysis of MAO–anion interactions impossible.

As can be seen from FT-IR spectra, the reaction progressing according to scheme depicted in Fig. 5 is not completed even at stoichiometric OH: Al–CH$_3$ groups ratio. The presence of the non-bonded PEGME is confirmed by FT-IR spectra, where bands of OH groups were observed for the same samples in which the presence of PEGME coordinated with salt but not bonded to the MAO nanocores was revealed by means of DSC experiments.
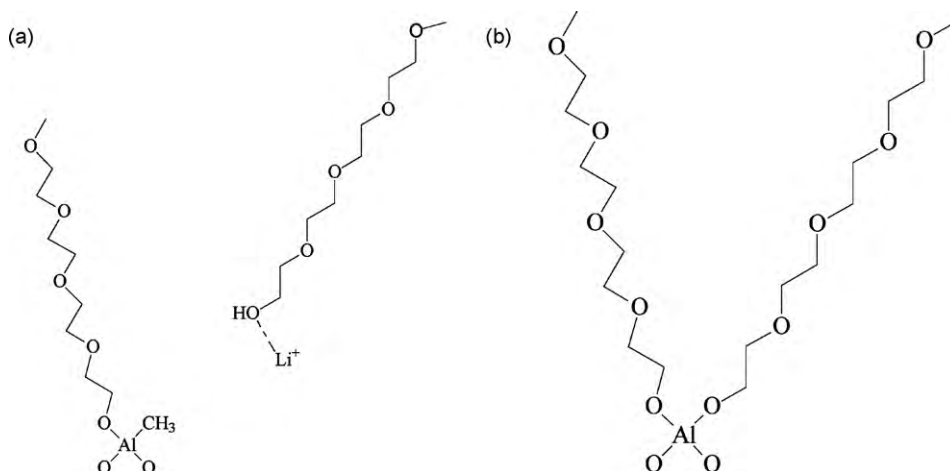

Fig. 6. Scheme of the reaction in the electrolyte. (a) Electrolyte constituents including still active Al–C bond and OH terminated PEG and (b) product of the reaction.

A comparison of FT-IR spectra of samples undoped and doped with LiCF$_3$SO$_3$ with the same MAO:PEGME ratio shows that hydroxyl groups consumption is more prominent in the absence of salt. This effect can be explained as a result preferred coordination of lithium cations by the hydroxyl groups oxygen and, therefore, hindered reaction of these groups with the MAO active sites. It is interesting to note that while comparing the spectra of freshly synthesized samples with those stored for six months we observe a further decrease of ν_{OH} band intensity in the spectra of the aged composites. This indicates that the reaction is still running in the annealed samples, probably due to the decreased (but still present) reactivity of Li$^+$ coordinated hydroxyl groups (see Fig. 6). A detailed look at these spectra reveals also some differences in conformation of polymer chains in LiCF$_3$SO$_3$ doped and undoped samples,

although the position of the ν_{COC} band, which is commonly used to analyze Li$^+$–PEO coordination remains practically unchanged.

In most cases, ν_{SO_3} bands of the triflate anion are used to study the salt dissociation process. However, in the PEO-based electrolytes the spectral region of both $\nu_{SO_3 \, sym}$ and $\nu_{SO_3 \, asym}$ vibrations is blurred by bands of the polymer. Therefore, we decided to focus on the analysis of the δ_{CF_3} band located at $\sim$750 cm^{-1}. According to the literature data, "free" anions and those belonging to the ionic pairs should give bands at 752 and 756 cm^{-1} respectively. In the sample without the MAO addition, only a single peak with maximum at 756 cm^{-1} was found in FT-IR spectra and no difference was observed upon comparison of the spectrum of a fresh sample with that registered for samples stored for one year. On the other hand, even a small amount of MAO involves significant change in the
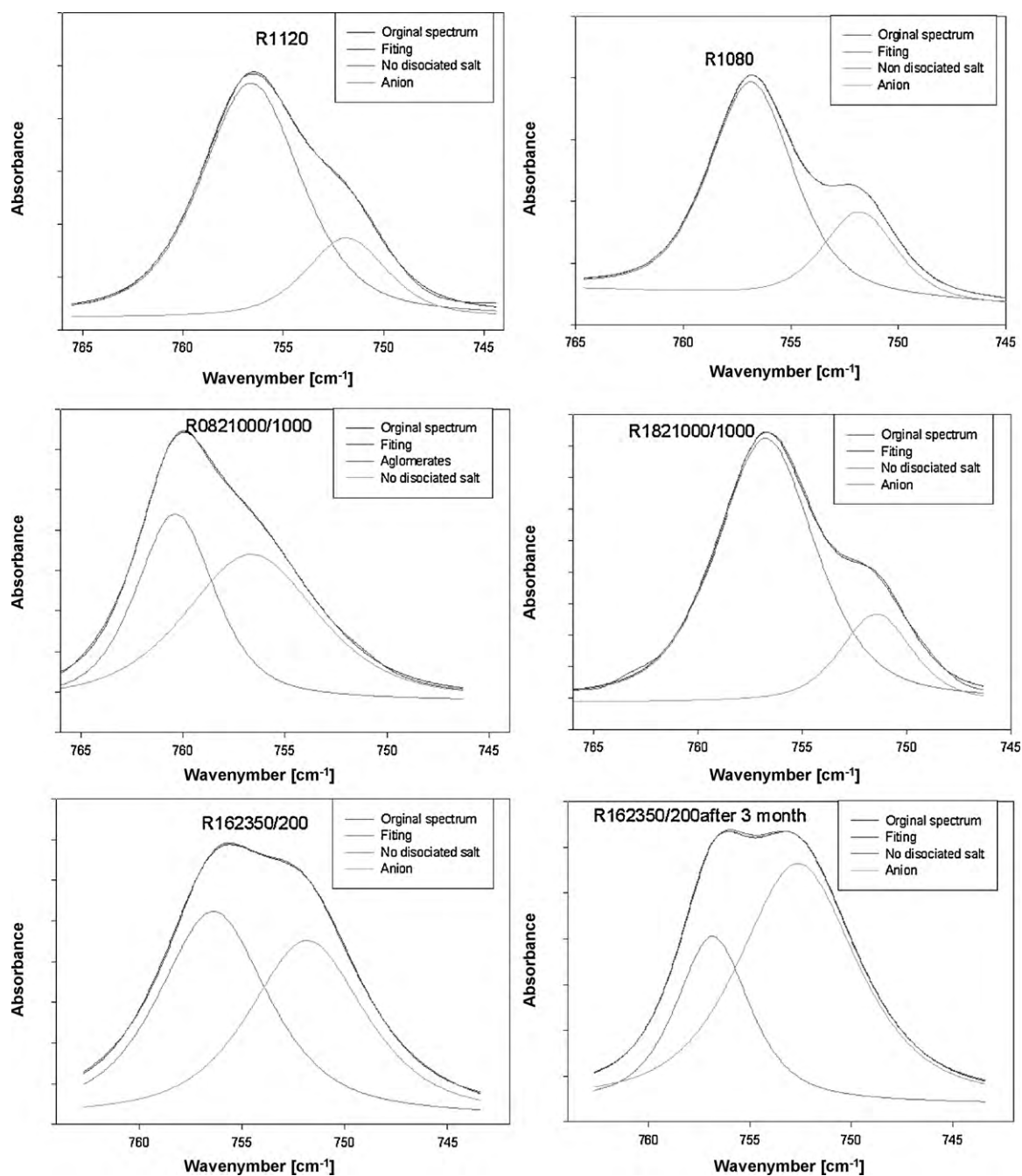

Fig. 7. Deconvolution of FT-IR spectral region correlated to the CF$_3$ symmetric deformation of anion. Constituents originating from free anions, non-dissociated salt and agglomerates were taken into consideration.

shape of the $\delta_{\text{sym CF}_3}$ band and an additional peak constituent (or a shoulder) attributed to "free" anions at 752 cm^{-1} is easily observed. The results of the deconvolution of $\delta_{\text{sym CF}_3}$ band are shown in Fig. 7. The typical spectra of electrolyte is shown in Fig. 8.

3.3. DSC studies

A set of the DSC traces for the studied electrolytes is shown in Fig. 9. The shape of the registered trace depends on sample composition. Some representative cases will be discussed here to reveal the correlations between sample composition and its thermal properties. Firstly, for crosslinked samples with 8 or 10 exchanged –CH$_3$ moieties (per MAO core) a completely amorphous system is observed revealing T_g about −60 °C. In this case the samples contained above 18 wt% of MAO cores and the same trace was observed independently of the consistence of a particular sample (rubbery or solid) and their composition differed. Presented samples were obtained in reaction of methylalumoxane with PEGME 350 with the addition of PEG 200 as the crosslinking agent. For the branched systems the thermal properties strongly depends on molar ratio of substrates. For the sample R1180 a completely amorphous system is observed revealing T_g about −60 °C. Contrastively, in the case of blended electrolyte (sample II T2) thermal properties of the system are determined by a large amount of PEGDME M_w = 500 g mol^{-1} present in the system. A small exothermic signal is observed at −36.7 °C corresponding to the sample crystallization and an endothermic transition with large heat consumption is observed here at 7.7 °C corresponding to the crystalline phase melting. In this case T_g value is equal to −64.2 °C being characteristic for all the blended samples containing lithium triflate. The values observed are slightly different from those reported in Ref. [21] for pure PEGDME–LiClO$_4$ systems revealing T_g = −56 °C and T_m = −12 °C as well as composites containing mechanically dispersed Al$_2$O$_3$ for which T_g = −62 °C and T_m = −10 °C. This difference can be attributed to the MAO nanocore interaction with the oligoether chains.

3.4. Conductivity studies

The comparison of the thermal conductivity) dependencies (see Figs. 10–13) shows that in ambient and elevated temperatures the blended system reveals a slightly better ionic transport. This observation can be correlated with lower viscosity of the systems containing a non-bonded oligomer and, thus, to increased
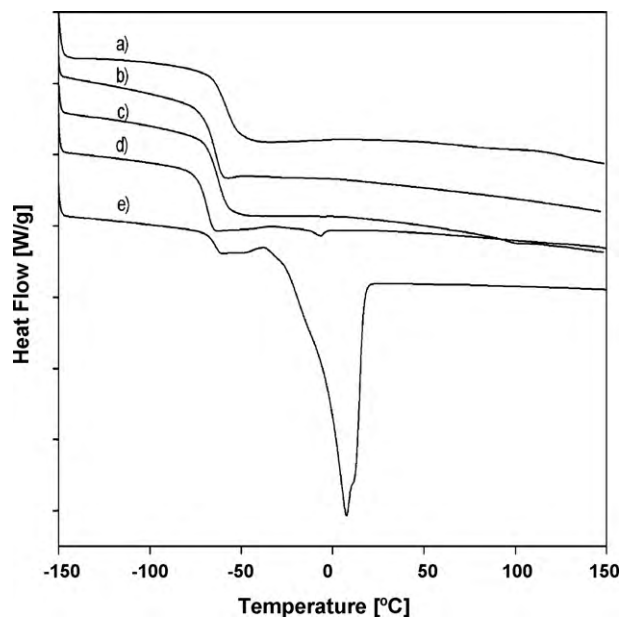

Fig. 9. DSC traces for heterocomposite electrolytes originating from the reaction of the MAO molecule with oligoglycols: (a) R142350/300, (b) R11080, (c) R162350/300, (d) R11120, and (e) II T5.

segmental mobility. Contrastively, in temperatures below 283 K the pristine branched system reveals higher conductivity values in comparison with the blended one. This phenomenon can be attributed to phase transition occurring in PEGDME 500 around 13 °C leading to its solidification of electrolyte. Therefore in this temperature range a step type decrease of conductivity is observed for systems containing PEGDME. This observation stays which is contrast with the behavior of the crosslinked samples where short oligoethers chains are coordinated by MAO molecule. In this case rather flat temperature dependence of the conductivity in the low temperature range is observed due to the elimination of the stiffening of the electrolyte originating from the phase transition. On the other hand these systems are of higher viscosity. This observation can be confirmed by the DSC data. In the case of the branched ones a slow monotonic decrease of conductivity is observed for the whole temperature range. The shape of the curves suggests the VTF type of conductivity behavior which corresponds nicely with the
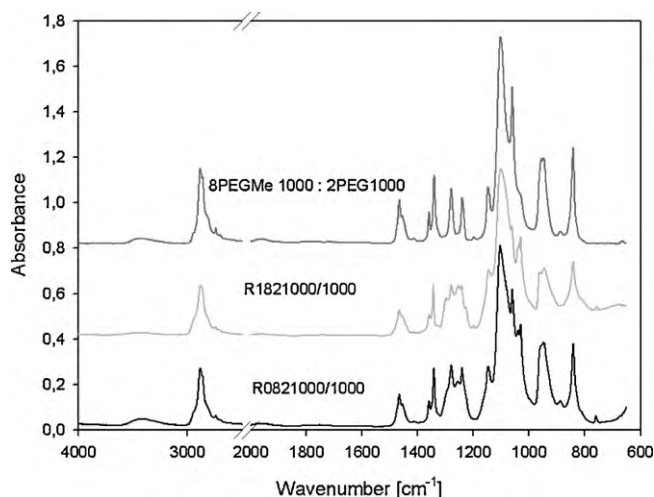

Fig. 8. FT-IR spectra of samples based on polyethylene glycol M_w = 1000 without salt, with salt and with salt and MAO.
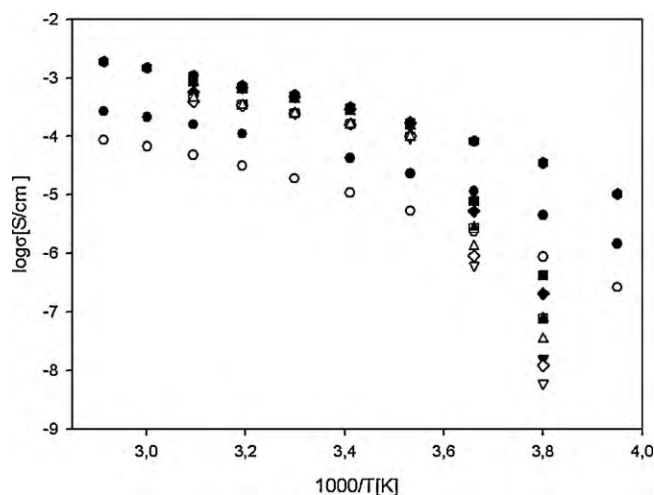

Fig. 10. Thermal dependences of conductivity for non-crosslinked MAO-based heterocomposite electrolytes: (●) R11120, (○) R1180, (▼) II P2, (♦) I P2, (□) II T2, (▽) I T2, (■) II P5, (⬤) OD100, (▲) I P5, (△) I T5, and (◇) I T2.
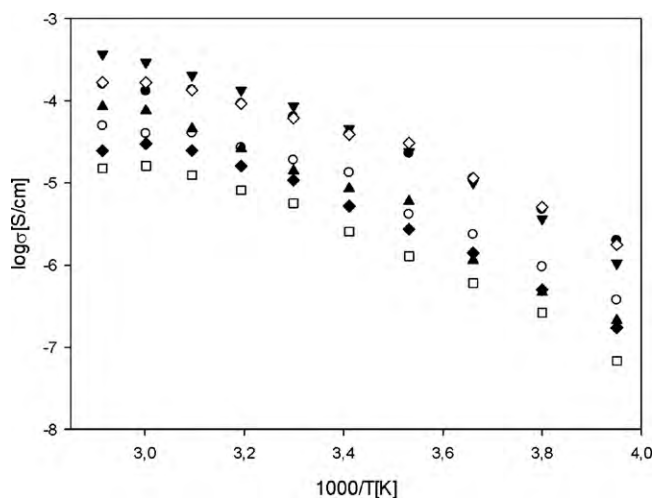
Fig. 11. Thermal dependences of conductivity for crosslinked MAO-based hetero-composite electrolytes: (●) R162350/300, (○) R142350/300, (▼) R182350/300, (♦) R162750, (◇) R142750, (▲) R162350/200, and (□) R142350/200.
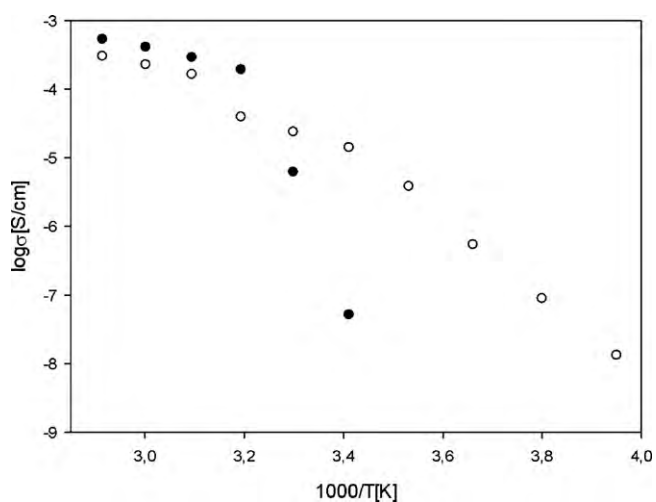

Fig. 12. Thermal dependences of conductivity for crosslinked MAO-based hetero-composite electrolytes: (●) R0821000/1000 and (○) R1821000/1000.
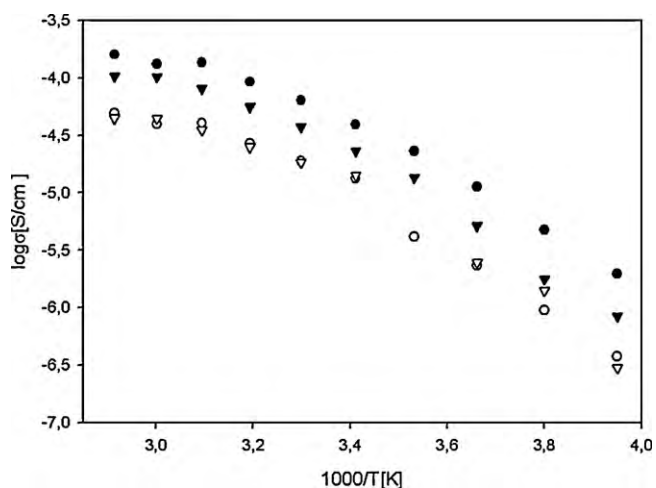

Fig. 13. Thermal dependences of conductivity for samples measured just after synthesis: (●) R162350/300 and (○) R142350/300, and after three months: (▼) R162350/300 and (▽) R142350/300.
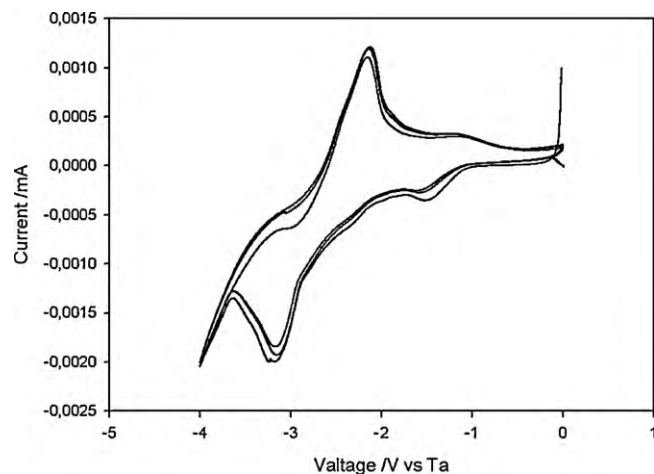

Fig. 14. Cyclic voltammogram of branched hybrid polymer electrolyte (1MAO:6PEGME 350 1 mol LiTF kg^{-1} of oligomer) on golden electrode at room temperature.

fully amorphous structure of these samples confirmed by DSC measurements. The comparison of the conductivity values observed for samples R11080 and R11120 reveals that the presence of non-bonded PEGME molecules in the later one (confirmed by the DSC and FT-IR measurements) leads to a conductivity increase in whole conductivity range. This can be correlated with the improved salt dissociation process observed in samples containing free –OH moieties (confirmed by FT-IR experiments). Unfortunately, this type of samples has no practical application because of the reactivity of PEGME molecules against the lithium electrode.

In the case of crosslinked systems conductivity is not strongly correlated with sample consistency (see Fig. 11). The highest conductivity values were observed for the liquid-like sample R182350/300 while the second best conductive one were the solid rubbery like materials R162350/300 and R142350/200. The obtained improvement of mechanical properties upon reaction with MAO was much more prominent in comparison with the observed conductivity decrease. This observation is extremely significant for the solid sample containing oligoether characterized by $M_w = 1000\,\mathrm{g\,mol^{-1}}$ (R0821000/1000 and R1821000/1000) (see Fig. 12). In this case a reference sample (R0821000/1000) which does not contain MAO reveals higher conductivity only in elevated temperatures exceeding its melting point. (In this temperature range the sample containing MAO is still solid.) For lower temperatures (when both systems are solid) the sample containing MAO did not reveal such prominent conductivity decrease. This phenomenon can be also correlated with mentioned before coordination of oligoether chains by MAO molecule. In the situation in which a prolonged reaction is observed (leading to sample solidification) the conductivity values either remain unchanged (e.g. for R142350/300) or are slightly decreased (e.g. for R162350/300) probably due to phenomena related with viscosity increase (see Fig. 13).

Finally, for the blended samples the lithium transference numbers were measured by the use of DC-polarization technique (see Table 1). In the case of samples containing LiClO$_4$ the heterocomposite formation does not lead to the significant changes of this parameter while in the case of ones containing LiCF$_3$SO$_3$ the value is increased above 0.5 probably due to interactions of the anions with Al–O cores originating from MAO.

Also the cyclic voltammetric studies of the hybrid polymer electrolytes on golden electrode with scan speed 5 mV s^{-1} were done (Fig. 14). They confirmed good cyclability in potential range from 0 V to −4 V vs. tantalum electrode. Deposition and stripping peaks
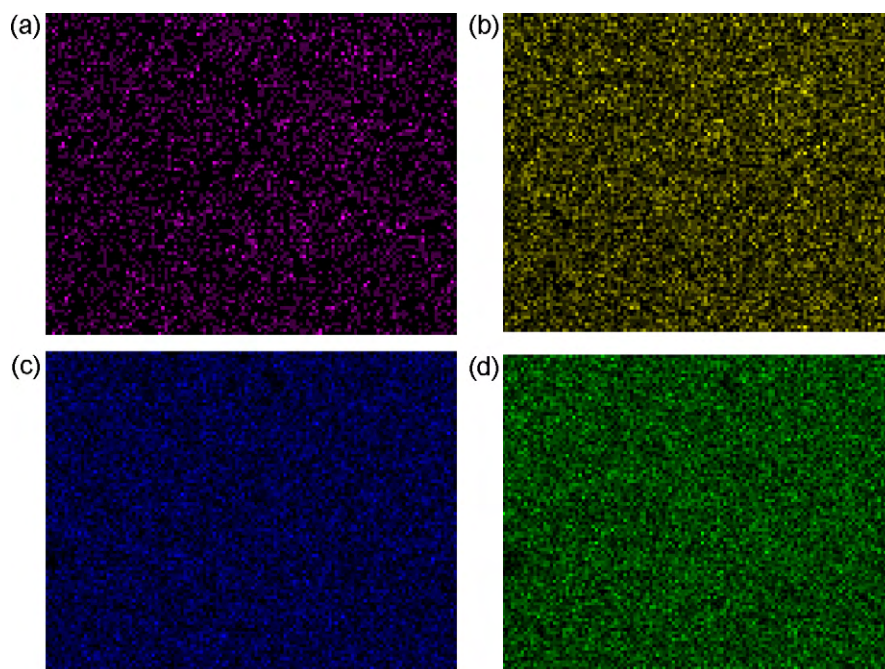
Fig. 15. EDX elementary mapping of the amorphous crosslinked hybrid polymer electrolyte: (a) distribution of S, (b) distribution of Al, (c) distribution of C, and (d) distribution of O for 5000× magnitude.

of lithium were observed in potential value close to −3.2 V and −2.2 V and decomposition of polymer matrix below 3.7 V. Further analysis is desirable to characterize the cyclic voltammetry plots. Thus the lower stability edge of the electrolyte is located below lithium plating/stripping range allowing the potential application in the lithium battery.

3.5. EDX studies

Morphology of crosslinked sample with composition 1MAO:4PEGME 350:2 PEG 200 with salt addition equal 1 mol kg^{-1} of polymer was analyzed. EDX analysis of hybrid polymer electrolyte confirmed uniform distribution of S (originating from salt), Al (inorganic part), C and O in the electrolyte. Full homogeneity of hybrid polymer electrolyte was proved, the results of the elementary mapping are shown in Fig. 15.

4. Conclusions

Firstly, we claim to have proved the formation of a new type of hybrid organic–inorganic composite polymeric electrolyte. The novelty here is based on the fact that the organometallic precursor used formed a nanosized Al–O cage itself. Thus, in consequence, a system was created being intermediate between typical nanocomposites with mechanically dispersed filler grains and materials obtained previously [28] by the sol–gel type of reaction. This system is characterized by electrical, thermal and mechanical properties which can be easily tailored by an appropriate choice of branching and crosslinking oligoglycols, molecular weight and molar ratio between nanocores and both reactants. We can obtain a fully amorphous and homogenous system if short chains are used or partially crystalline in the case of applying longer ones. FT-IR experiments reveal slightly improved salt dissociation in the electrolyte containing MAO whose properties can be correlated with improved cationic transference numbers measured for electrolytes containing LiTf. On the other hand the salt dissociation is also promoted by the free non-bonded –OH moieties present in some of the studied samples (which not the issue of the conducted study). Addi-

tionally, an influence of salt on the process of matrix formation was observed. The chemical reaction of MAO with oligoglycols is inhibited by the presence of the salt probably owing to complex formation occurring between MAO and LiTf. Nevertheless, the long time observation proved that after some weeks of storage the completion of the reaction is achieved.

References

[1] F.M. Gray, Solid Polymer Electrolytes. Fundamentals and Technological Applications, VCH Publishers, Weinheim, 1991.
[2] B. Scrosati, G. Stienen (Eds.), Applications of Electroactive Polymers, Kluwer Academic Publishers, 1993.
[3] P.D. Bruce, Solid State Electrochemistry, Cambridge University Press, 1995.
[4] J.R. MacCallum, C.A. Vincent (Eds.), Polymer Electrolyte Reviews 1 and 2, Elsevier, Amsterdam, 1987.
[5] J.M. Tarascon, M. Armand, Nature 44 (2001) 359.
[6] M. Watanabe, A. Nishimoto, Solid State Ionics 79 (1995) 306.
[7] F. Alloin, D. Benrabah, J.-Y. Sanchez, Journal of Power Sources 68 (1997) 372.
[8] H. Cheradame, J.-F. Lenest, A. Gandini, M. Leveque, Journal of Power Sources 14 (1985) 27.
[9] F. Croce, G.B. Appetecchi, L. Persi, B. Scrosati, Nature 394 (1998) 456.
[10] J. Przyłuski, Z. Florjańczyk, K. Such, H. Wyciślik, W. Wieczorek, Synthetic Metals 35 (1–2) (1989) 241.
[11] W. Wieczorek, K. Such, J. Płocharski, J. Przyłuski, in: B. Scrosati (Ed.), Proc. II Int. Symposium on Polymer Electrolytes, Sienna, 1989, Elsevier Applied Science, London, New York, 1990, p. 339.
[12] S. Skaarup, K. West, B. Zachau-Christiansen, Solid State Ionics 28–30 (1988) 979.
[13] J. Zhou, P.S. Fedkiw, Solid State Ionics 3–4 (2004) 275.
[14] J. Płocharski, W. Wieczorek, J. Przyłuski, K. Such, Applied Physics A: Solids and Surfaces 49 (1989) 55.
[15] M. Popall, H. Durand, Electrochimica Acta 37 (1992) 1593.

[16] A. Sitarek, P. Rajewski, G. Żukowska, H. Wyciślik, M. Ciosek, M. Siekierski, Materials Science-Poland 24 (2006) 213.
[17] M. Popall, M. Andrei, J. Kappel, J. Kron, K. Olmaa, B. Olsowskia, Electrochimica Acta 43 (1998) 1155.
[18] S.C. Nunes, V. de Zea Bermudez, M.M. Silva, M.J. Smith, E. Morales, R.A. Sá Ferreira, L.D. Carlos, J. Rocha, Solid State Sciences 12 (2006) 1484.
[19] M.M. Silva, S.C. Nunes, P.C. Barbosa, A. Evans, V. de Zea Bermudez, M.J. Smith, D. Ostrovskii, Electrochimica Acta 52 (2006) 1542.
[20] P.C. Barbosa, M.M. Silva, M.J. Smith, A. Gonçalves, E. Fortunato, Electrochimica Acta 52 (2007) 2938.
[21] S.C. Nunes, V. de Zea Bermudez, D. Ostrovskii, P.B. Tavares, P.C. Barbosa, M.M. Silva, M.J. Smith, Electrochimica Acta 53 (2007) 1466.
[22] M. Vittadello, S. Suarez, S.H. Chung, K. Fujimoto, V. Di Noto, S.G. Greenbaum, T. Furukawa, Electrochimica Acta 48 (2003) 2227.
[23] M. Armand, C. Poinsignon, J.-Y. Sanchez, V. de Zea Bermudez, US Patent, 5,283,310 (1994).
[24] K. Onishi, M. Matsumoto, Y. Nakacho, K. Shigehara, Chemistry of Material 9 (1996) 469.
[25] K. Matsushita, Y. Shimazaki, M.A. Mehta, T. Fujinami, Solid State Ionics 133 (2000) 295.
[26] V. Di Noto, V. Zago, Journal of The Electrochemical Society 151 (2004) A216.
[27] H. Peterlik, H. Rennhofer, V. Torma, U. Bauer, M. Puchberger, N. Husing, S. Bernstor, U. Schubert, Journal of Non-Crystalline Solids 353 (2007) 1635.
[28] Z. Florjańczyk, E. Zygadło-Monikowska, W. Bzducha, Electrochimica Acta 45 (2000) 1203.
[29] E. Zygadło-Monikowska, Z. Florjańczyk, E. Rogalska-Jońska, A. Werbanowska, A. Tomaszewska, N. Langwald, D. Golodnitsky, E. Peled, R. Kovarsky, S.H. Chung, S.G. Greenbaum, Journal of Power Sources 173 (2007) 734.
[30] M.S. Siekierski, M. Marczewski, 211th Meeting of the Electrochemical Society, Chicago, USA, May, 2007.
[31] V. Di Noto, V. Zago, G. Pace, M. Fauric, Journal of The Electrochemical Society 151 (2004) A224.
[32] Y. Masuda, M. Nakayama, M. Wakihara, Solid State Ionics 178 (2007) 981.
[33] Y. Masuda, M. Seki, M. Nakayama, M. Wakihara, H. Mita, Solid State Ionics 177 (2006) 843.
[34] Z. Florjańczyk, E. Zygadło-Monikowska, W. Bzducha, Electrochimica Acta 45 (2000) 1203.
[35] M. Piszcz, A. Plewa-Marczewska, G.Z. Żukowska, A. Pietrzykowski, M. Siekierski, Electrochimica Acta 55 (2010) 1338.
[36] A. Pietrzykowski, T. Skrok, S. Pasynkiewicz, T. Radzymiński, K. Suwińska, XVth FECHEM Conference on Organometallic Chemistry, Zürich, 2003.
[37] B.A. Boukamp, Solid State Ionics 10 (1986) 31.
[38] P.G. Bruce, C.A. Vincent, Journal of Electroanalytical Chemistry and Interfacial Electrochemistry 225 (1987) 1.
[39] Y. Dai, Y. Wang, S. Bajue, S.G. Greenbaum, D. Golodnitsky, G. Ardel, E. Strauss, E. Peled, Electrochimica Acta 43 (1998) 1557.
[40] G. Negasuramanian, E. Peled, A.I. Attia, G. Halpert, Solid State Ionics 67 (1993) 51.